PONTIFICIA UNIVERSIDAD CATOLICA DE CHILE
ESCUELA DE INGENIERIA

EFFICIENT SIMULATION OF ACCELERATIONS DURING CURVE NEGOTIATION USING A STEWART PLATFORM

JOSÉ TOMÁS ARENAS DONOSO

Thesis submitted to the Office of Research and Graduate Studies in partial fulfillment of the requirements for the Degree of Master of Science in Engineering.

Advisor:
LUCIANO E. CHIANG SÁNCHEZ

Santiago de Chile (August, 2011)

© 2010, José T. Arenas-Donoso

PONTIFICIA UNIVERSIDAD CATOLICA DE CHILE
ESCUELA DE INGENIERIA

EFFICIENT SIMULATION OF ACCELERATIONS DURING CURVE NEGOTIATION USING A STEWART PLATFORM

JOSÉ T. ARENAS DONOSO

Members of the Committee:

LUCIANO CHIANG SÁNCHEZ

MIGUEL TORRES TORRITI

JOSÉ REYES AROCA

MICHEL VAN SINT JAN

Thesis submitted to the Office of Research and Graduate Studies in partial fulfillment of the requirements for the Degree of Master of Science in Engineering.

Santiago de Chile (August, 2011)

To all my loved ones, who always have motivated and supported me in my projects.

ACKNOWLEDGEMENTS

I would like to thank the many actors that supported, helped and guided me through this work that represents an important moment in my professional and personal career.

First, to my family and friends who have always supported me with love and encouraged me every day to achieve my goals. Also, to the people who is part of the Mechanical and Metallurgical Engineering Department at Pontificia Universidad Católica de Chile that helped me during the most important part of my research and assisted me with their advice and experience. Finally, a special acknowledge to Professor Luciano Chiang for his mentoring during my time in the university and particularly in this research as part of my Master Degree program.

CONTENTS

LIST OF TABLES

LIST OF FIGURES

Page

ABSTRACT

This work intends to contribute to studies using driving simulators which can benefit from having a simple and efficient methodology to integrate motion as part of the simulation. In order to achieve this, a motion cueing algorithm dedicated to simulate characteristic low frequency lateral accelerations of a vehicle during curve negotiation is developed and tested using a Stewart platform.

Three experiments were carried out to test the physical validity of the proposed methodology and to assess the overall performance of the simulation system.

Results showed that: (1) physical validity was achieved since errors between resultant and reference accelerations ranged in orders of 10^{-2} g in all three experiments, and (2) effective spectrum of simulation can be enhanced when downscaling the input signal and using higher tilt rates than traditional 3°/s.

This method can be replicated to complement researches addressing car driving with simulators, being suitable for achieving more elaborated movements to support sensorial immersion during simulation.

Keywords: motion cueing, driving simulator, Stewart platform, tilt coordination.

RESUMEN

La intención de este trabajo es contribuir a los estudios que se realizan utilizando simuladores de manejo de manera que puedan beneficiarse al contar con una simple y eficiente metodología para integrar el movimiento como parte de la simulación. Para esto, un algoritmo de movimiento dedicado a simular las aceleraciones de baja frecuencia características de un vehículo en curva es desarrollado y probado utilizando una Plataforma de Stewart.

Se realizaron tres experimentos para probar la validez física de la metodología propuesta y para evaluar el desempeño general del sistema de simulación.

Los resultados mostraron que: (1) se consiguió la validez física dado que los errores entre las aceleraciones resultantes y de referencia se mantuvieron en el orden de los 10^{-2} g en los tres experimentos, y (2) el espectro efectivo de simulación puede ser aumentado cuando se escala la señal de entrada y se utilizan mayores tasas de inclinación que la tradicional de 3°/s.

Este método puede ser replicado para complementar estudios que aborden el manejo de vehículos con simuladores, siendo adecuado para lograr movimientos más elaborados que aporten a la inmersión sensorial durante la simulación.

Palabras Claves: señales de movimiento, simulador de manejo, plataforma de Stewart, coordinación por inclinación.

I. INTRODUCTION AND BACKGOUND

I.1 Motivation

Nowadays, there is a great variety of applications that can benefit from a simulator. This depends on its capability to render the most complete and accurate sensorial experience for the user considering visual, hearing, haptic and vestibular inputs.

Simulators have motion devices in order to reproduce the acceleration inputs. There is a challenge performing the movement to consequently deliver a high fidelity experience of the event that is being simulated. Limited workspace of motion based simulators makes it difficult to render the whole spectrum of motion. Motion cueing algorithms usually address part of this problem taking advantage of the ambiguities that occurs in the vestibular system.

Under this perspective, this work intends to contribute on developing, in a simple way, a method to successfully render a particular car driving event under the constrained workspace of a traditional motion device: the Stewart Platform.

I.2 Hypothesis and approach

The hypothesis of this work is that a significant contribution on driving simulation can be achieved by a motion methodology based on tilt coordination when simulating characteristic low frequency accelerations of a car.

The approach is to facilitate and contribute to the validity of studies with driving simulators which can benefit from having a simple and efficient methodology to integrate motion as part of the simulation.

I.3 Objectives and expected results

The main objective of this work is to synthesize the movement of a Stewart Platform to render characteristic low frequency lateral accelerations of a car during curve negotiation.

The specific objectives are:

a) Develop a methodology based on the tilt coordination method to produce the desired acceleration using a Stewart Platform.
b) Experimentally test the physical validity of the methodology.

The expected result of this work is a simple, reliable and straightforward methodology to process a desired acceleration input to be rendered by the Stewart Platform motion.

I.4 Background

I.4.1 The Stewart Platform

The mechanism known as the Stewart Platform (SP) is a six degree of freedom (DOF) parallel manipulator originally proposed by Stewart (1965) as a flight simulator consisting in three extensible legs supporting a triangular platform. In one communication in response to Stewart's paper, Gough (1965) suggested the use of six parallel linear actuators as used for the tyre test machine proposed with Whitehall in 1962 (Gough & Whitehall, 1962). Nowadays, the mechanism is referred as the Stewart-Gough Platform crediting both for the invention, but it is mainly known by Stewart's name because of the popularity of his paper (Dasguptaa & Mruthyunjaya, 2000).

Figure I.1 shows one of the most traditional kinematic structures known as the 6-UPS Stewart Platform in which the legs are connected to a base frame with universal joints and with spherical joints to a moving platform. The six DOF of the platform are driven by the length of the six prismatic joints of the legs.

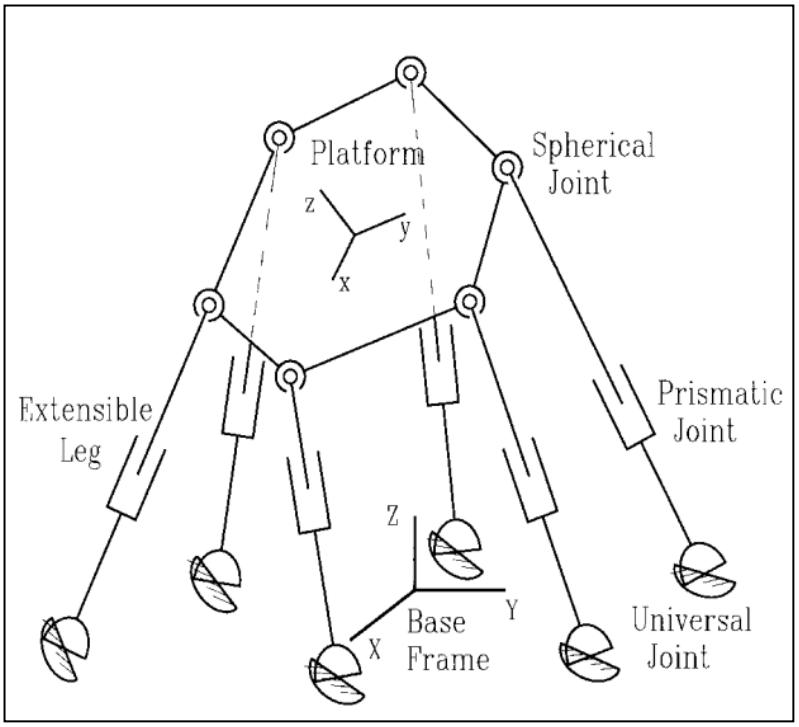

Figure I.1: One traditional structure of the Stewart Platform showing the types of connections of the extensible legs (illustration from Dasguptaa & Mruthyunjaya, 2000).

Mechanical manipulators have been vastly studied from different approaches. Theory has established a series-parallel manipulators duality, with significant differences between these two kinds of mechanisms (Dasguptaa & Mruthyunjaya, 2000). Parallel manipulators have straightforward inverse kinematics and direct dynamics, but complicated direct kinematics and inverse dynamics. In contrast, series manipulators exhibit just the opposite.

The direct or forward kinematics problem is, given the lengths of the 6 legs, to determine the position and orientation of the moving platform. Extensive works on this field have been conducted using numerical and analytical approaches, for example: Nanua et.al. (1990) reduced the direct kinematics to a 16th-order polynomial equation, Liu et al. (1993) proposed an algorithm that involves solving only three nonlinear simultaneous equations and Jakobovic & Budin (2002)

developed sophisticated mathematical representations with optimization algorithms for a solution in real-time conditions.

The inverse kinematics approach is usually utilized for control consisting in determining the lengths of the legs given a set of DOF. Work done by Indrawanto (2009), Chiew et al. (2009) and Lee et al. (2003) covers computational control of the platform. PID and Sliding Mode Control are the two most used control methods for the SP depending on the characteristics of the actuators.

Different formulations are reported in literature for dynamics analysis: Newton-Euler (Guo & Li, 2006), Lagrange (Lin & Chen, 2009), virtual work principle (Huang et al., 2004) and Kane equations (Liu et al., 2000); however, this field has many open problems to solve. Computational support is also widely used due to its complexity

Other research lines aim for an optimal design of the SP: implications of design parameters (Huang et al., 1999; Hostens et al., 2005), workspace determination (Ay et al., 2009; du Plessis, 1999), and singularities that occur in some configurations causing the manipulator to collapse (Hua et al., 2007).

Many authors have suggested the use of this mechanism for a variety of tasks considering its advantages as a parallel manipulator: good dynamic performance, high load capacity and precise positioning. Being the most used parallel manipulator (Peña et al., 2002), actual applications for the Stewart Platform vary in fields as robotics, automation, astronomy, vibration control, sensing devices, simulation and medicine.

Some interesting conducted works are:

i) A simulator to study human gait, aiding in the diagnosis and rehabilitation of patients with motor injuries (Sevillano et al., 2008).

ii) A master-slave manipulator to study bilateral force on servo control strategies (Zhang et al., 2007).

iii) A single-stage active vibration isolator for precision manipulation of payloads (Preumont, et al., 2007).

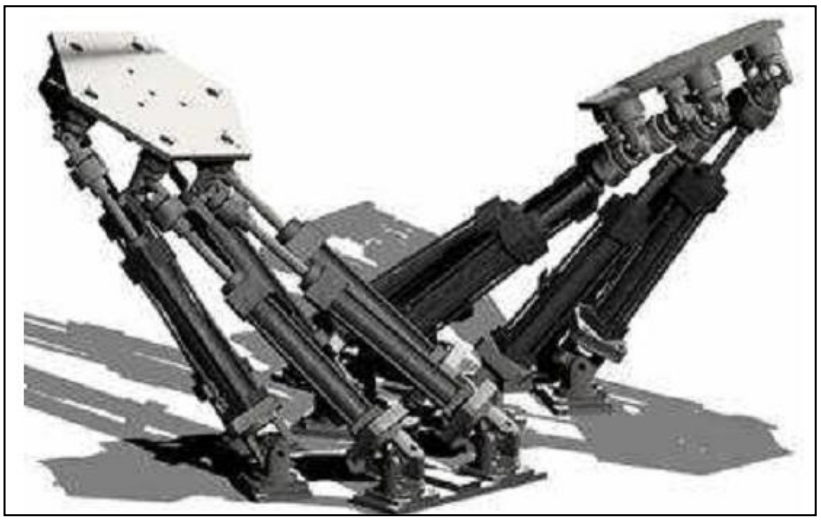

Figure I.2: Gait simulator using two Stewart Platforms (illustration from Sevillano et al., 2008).

I.4.2 Vestibular system

The vestibular system has both sensor and motor functions. As a sensor system, it provides information of movement and balance by detection of linear and rotational motion. As a motor system it has a role in posture control orienting to the vertical, controlling center of mass, and stabilizing eye movement allowing clear vision when the head is in motion.

The vestibular system is located in the inner ear and it is composed by the semicircular canals, which indicates rotational movements and the otoliths organs, the saccule and utricle, which indicate linear accelerations. Figure I.3 shows the location of the vestibular system in the inner ear and its components.

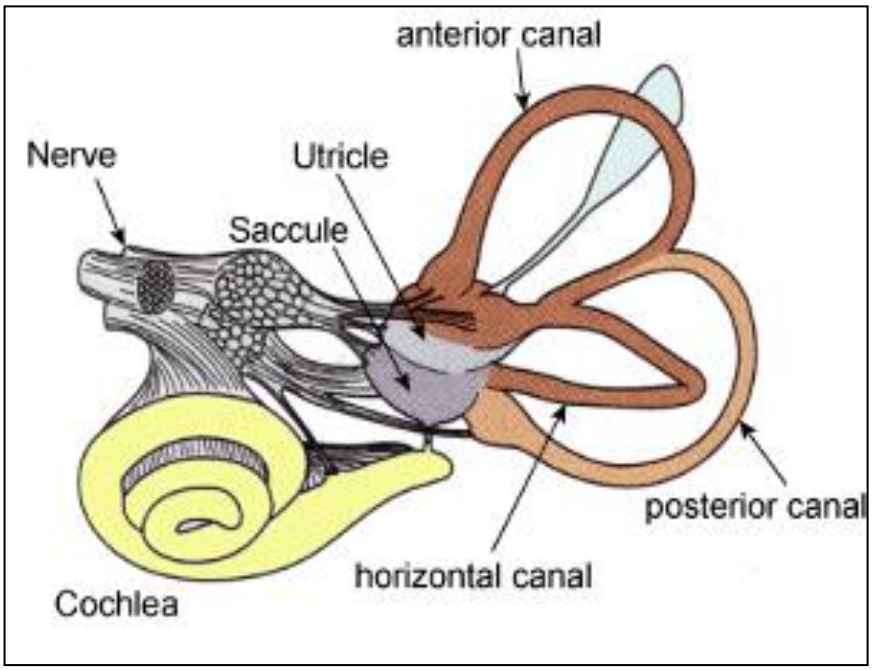

Figure I.3: Vestibular organs in the labyrith of the inner ear (retrieved july 2011, from http://en.wikipedia.org/wiki/Vestibular_system).

Three semicircular canals are filled by the endolymph fluid and are approximately orthogonal to each other to detect rotations. Movement and inertia of this fluid stimulate hair cells that transduct the mechanical movement to nervous signals proportional to head velocity over the common range of frequencies in which the head moves. The two otolith organs are associated with semicircular canals providing information about linear acceleration and head tilt with respect to gravity. Because of their orientation, the utricle is sensitive to a change in horizontal motion, and the saccule to vertical acceleration. They also trigger neural stimuli by

stimulation of hair cells. In general, semicircular canals respond to high frequency movements, while the otoliths organs to low frequency.

There is an ambiguity between gravity and linear accelerations for the otolith organs so tilt can be sensed as linear acceleration. This happens whenever there is a mismatch between internal estimation of gravity and the physiological measurement of the gravitoinertial force (Merfeld et al., 1999). It has been demonstrated that the central nervous system resorts on semicircular canals and vision to resolve this ambiguity of tilt and translational linear acceleration (Wood & Reschke, 2007).

Benson (1990) has summarized interesting findings of several researchers about vestibular system thresholds. The threshold for detection of tilt from the vertical is on the order of 2°. For angular motion perception, the mean threshold about the z axis is about 0.32°/sec. Threshold for linear acceleration has been found to range from 0.002 to 0.027 g. Transient movements shorter than 10 seconds with a little change in angular velocity (< 2°/sec) or acceleration below 0.05 m/sec2, may be undetected.

Mathematical models of the vestibular system and applications concerning the knowledge of its behavior are supporting the simulation industry. Merfeld, et al. (1999) investigate the brain internal models to help estimate linear acceleration and gravity. Reymond et al. (2002) describe a computational model for the sensory perception of self-motion used for the analysis of complex sensory interactions. Figure I.4 shows which variables are taken in count for modeling the system response: head acceleration A, gravity G, gravitoinertial acceleration F, linear velocity V and angular velocity Ω.

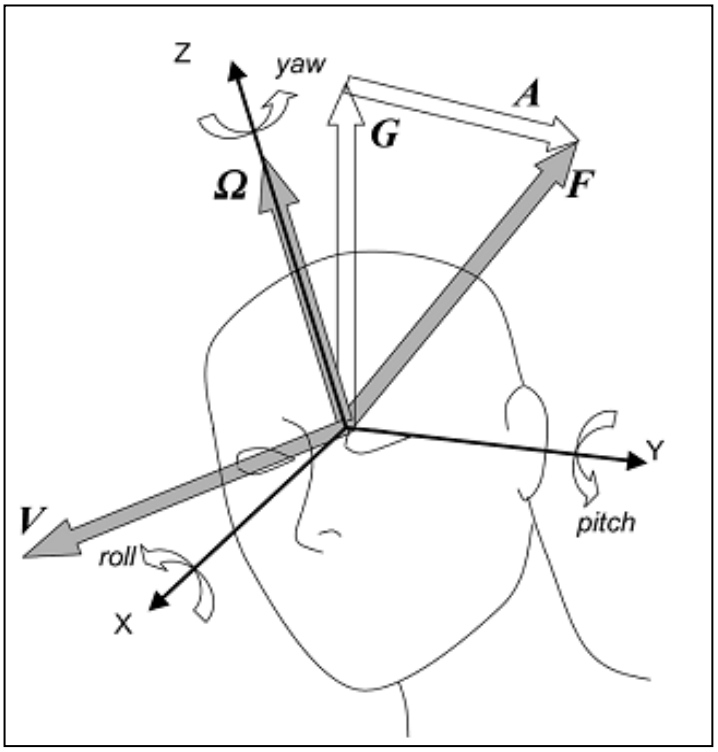

Figure I.4: Modelling of the vestibular system response (illustration from Reymond et al., 2002).

I.4.3 Driving simulators

The first driving simulator was built by Volkswagen in the early '70s and consisted of three actuated DOF. In the '90s appeared the first six DOF actuated simulator from Daimler-Benz and throughout that decade, several simulators with similar characteristics were built by FORD, JARI, BMW, Renault, WIVW and Nissan (Slob, 2008). Through the years, electric servo technology has replaced hydraulic actuation due to developments concerning energy, control and versatility.

Three levels of fidelity can be identified for driving simulators as the human-in-the-loop condition increases. This is determined mainly by the DOF of the cabin, the quality of visual system and the coherence of the whole (Slob, 2008). Low-level simulator consists in a car seat, preferably inside a car, fixed to the ground looking

to a fixed screen. For mid-level driving simulators, the car has one degree of freedom, usually rotation, and the screen can be fixed or move along with the movement of the car. A high-level simulator moves the cabin in 6 DOF and redundant DOF are used to allow longer planar excursions and prolonged accelerations as can be seen on Figure I.5.

Figure I.5: Toyota high-level driving simulator (retrieved july 2011 from http://www.zercustoms.com/news/Toyota-Driving-Simulator.html).

Driving simulators are applicable in tasks such as design and evaluation of vehicles (Freeman, et al., 1995), monitoring driver behavior (Brookhuis & de Waard, 2010; Auberlet et al., 2010), studying human-machine interaction (Mulder et al., 2008) and assessing road design (Charlton, 2004; Comte & Jamson, 2000). The most important advantage using a simulator is the capability to recreate any driving condition under a safe environment without significant costs. This allows the study and monitoring of risky, complex and infrequent situations or scenarios all the times needed. The advantages of the latter become evident when researching with elder

subjects (Shanmugaratnam et al., 2010; Lee et al., 2003) and when exposing the drivers to hazardous driving conditions (Coutton-Jean et al., 2009).

The main drawback when using a motion based driving simulator is the limited workspace of the standard motion devices as the Stewart Platform (Kim et al., 1997). This basic constraint of limited actuator stroke necessarily affects the validity of motion cueing (Reymond & Kemeny, 2000) and do not enable a one-to-one feedback (Colombet et al., 2008). Therefore, it is very important to develop techniques to exploit the workspace of the motion device and believably simulate large trajectories using smaller movements (Berger et al., 2010).

Even when driving simulators are considered a cost effective tool to carry out representative experimentations (Kemeny, 2001), they do not perfectly replicate the motion characteristics of a vehicle and the subject must depend on the simulator fidelity adapt correctly to the task (McGehee et al., 2004). In literature, it has been stated that only for advanced driving and handling skills motion is required (Bowen et al., 2006). In the end, the ultimate judge for the believability of a simulation experience is the human subject (Berger et al., 2010).

I.4.4 Motion cueing algorithms

Motion simulation is achieved by stimulation of the vestibular system which manages the information about linear and angular inertial accelerations of the body. Motion cueing algorithms aim to resemble real movements in simulator environments having to meet contradictory objectives: optimizing the motion rendering and keeping the motion device within its workspace (Colombet et al., 2008). Different algorithms are proposed for driving simulators according to this trade-off: classical, adaptive, optimal and predictive being the most common.

The most popular motion cueing algorithm is the Classical Washout Algorithm described in Figure I.*6*. This method is used to process an input to produce movement as well as keep the motion within the workspace of the system.

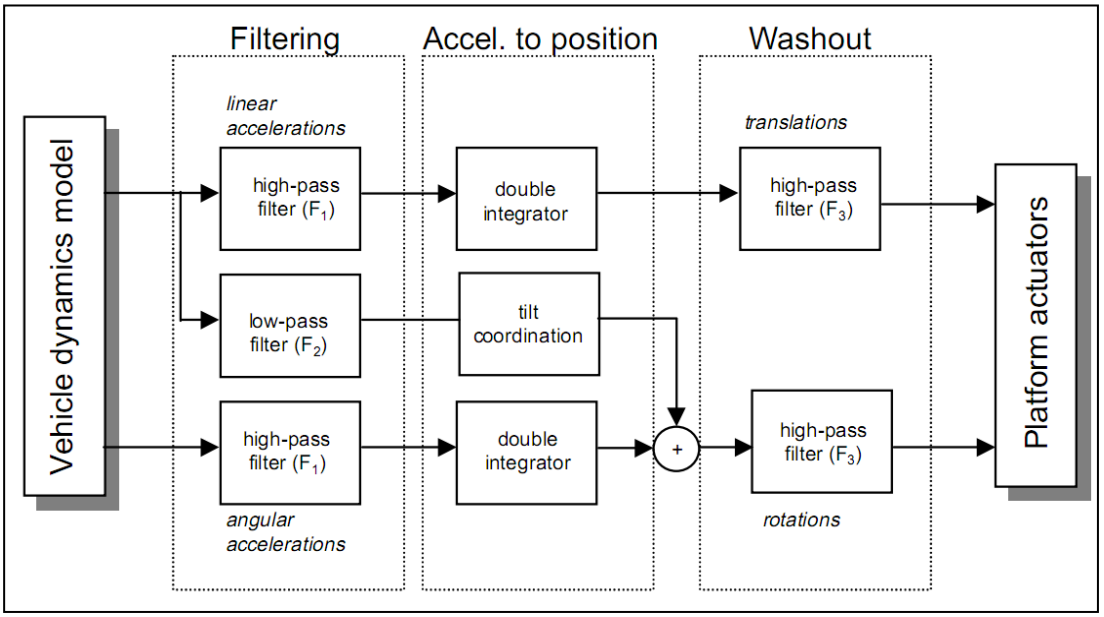

Figure I.6: Signal processing of the Classical Washout Algorithm to perform motion (illustration from Reymond & Kemeny, 2000).

Rendering low frequency accelerations in a limited workspace is achieved by the "tilt coordination" technique that takes advantage of the perceptual ambiguity between sustained linear accelerations and rotations of the body (Reymond & Kemeny, 2000; Kemeny, 1999; Ravichandran, 2010). The principle is to apply whole body tilt at a rate below a rotational threshold of typically 3°/s to create an illusion of linear self-motion acceleration due to the fraction of the gravity vector perceived by the otolith organs (Groen & Bles, 2004). Best results are achieved when consistent visual acceleration is presented together with tilt (Berger et al., 2010). Figure I.7 shows the principle used for tilt coordination based on how the vestibular system interprets a tilt as a linear acceleration.

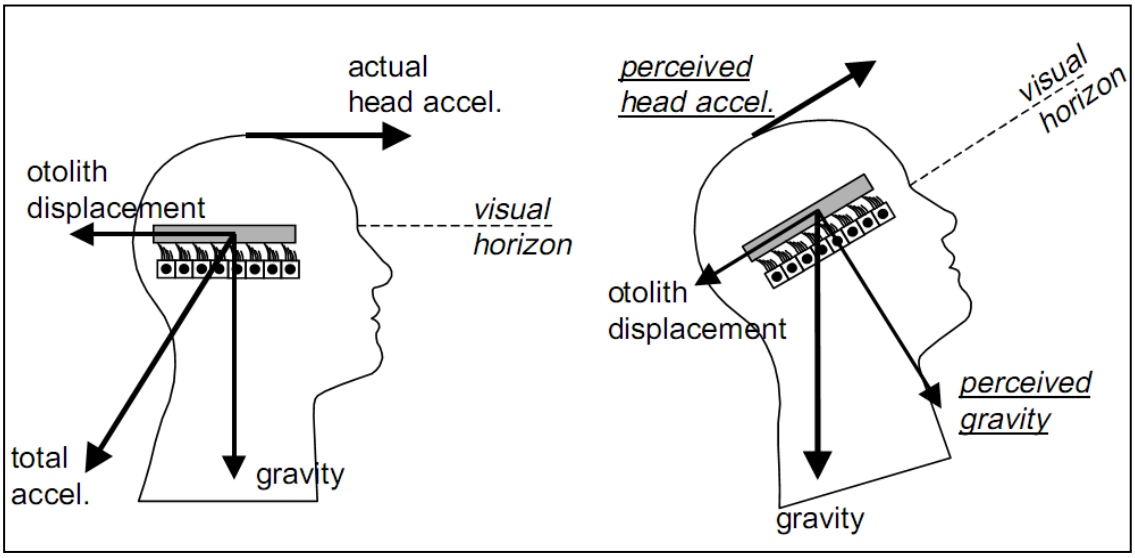

Figure I.7: Tilt coordination principle based on the ambiguity of the otolith organs (illustration from Reymond & Kemeny, 2000).

The need and validity of motion simulation is an on-going research. In the research done by Slob (2008), he mentions that the main reason to include motion cues is to prevent simulator sickness and to add more realistic workload on the driver. Other studies mention that it is essential to respect the characteristics the perception systems (Kemeny, 1999) because mismatch between expected and real sensations is probably one of the major causes of motion sickness (Harris, et al., 2001) and this conflict may cause the individual to become ill and so interfere with task performance (Bowen et al., 2006).

Furthermore, works done in motion and no-motion conditions concludes that significant differences exist affecting the results of the research. Study addressing the role of lateral acceleration in curves done by Reymond et al. (2001) and Greenberg et al. (2003) state that the difference in results are due to absence of extravisual sensory cues, e.g. motion cues. Another research focusing on braking and cornering tasks with and without motion cues reveals that motion prevented subjects from performing too unrealistic decelerations when braking and that lateral

and longitudinal cues influenced trajectory and linear velocity when cornering (Siegler et al., 2001). Other researchers report that the absence of physical motion in a driving simulator modifies the driver's reactions (Kemeny & Panerai, 2003) and that test subjects prefer dynamical to static simulation (Colombet et al., 2008).

Constant effort is done to develop, test and validate motion cueing algorithms to render realistic motion specially focusing in small workspace simulators (Valente-Pais et al., 2009; Damveld et al., 2010; Nehaoua et al., 2006).

II. EFFICIENT SIMULATION OF ACCELERATIONS DURING CURVE NEGOTIATION USING A STEWART PLATFORM

II.1 Introduction

Nowadays driving simulators are applicable in a broad range of applications as vehicle design (Kemeny, 2001), driver behavior research (Shanmugaratnam, Kass, & Arruda, 2010), human-machine interface studies (Mulder, Abbink, & Boer, 2008) and road design (Charlton, 2004). One important advantage when using a simulator is the capability to recreate driving conditions under a safe and controlled environment without significant costs, allowing to address risky, complex and infrequent situations or scenarios as many times needed (Brookhuis & de Waard, 2010; Coutton-Jean, Mestre, Goulon, & Bootsma, 2009). Furthermore, the use of a simulator allows investigating and monitoring one important factor related to driving: the role of the pilot, i.e. the effect of the human-on-the-loop.

Part of the quality of a simulator depends on its capability to render vestibular inputs. Even when the need and validity of motion in simulation is still an important investigation topic (Bowen, Oakley, & Barnett, 2006), several research efforts have concluded that motion cues play a significant role especially when other information is scarce (Greenberg, Artz, & Cathey, 2003) or, at least, have a positive contribution for perception of self-motion (Siegler, Reymond, Kemeny, & Berthoz, 2001) thus, improving task performance on the simulator (Kemeny & Panerai, 2003) and preventing sensory conflict that leads to motion sickness (Kemeny, 1999).

To perform these cues, simulators have motion devices in order to reproduce the acceleration effects while driving. The most popular of these devices is the Stewart Platform, a six degree of freedom (DOF) parallel manipulator originally proposed by Stewart (1965) as a flight simulator. Many authors have suggested the use of this mechanism considering its advantages as a parallel manipulator: good dynamic performance, high load capacity and precise positioning (Dasguptaa & Mruthyunjaya,

2000). The drawback of limited workspace makes it difficult to render the whole spectrum of characteristic driving cues (Kim, Lee, Park, Park, & Cho, 1997). Then, there is a challenge representing these cues to properly stimulate the user's sense of motion and balance to consequently deliver a high fidelity vestibular experience.

Motion cueing algorithms address the problem of maximizing the simulation capabilities of the motion device within its mechanical constraints and limitations (Colombet, Dagdelen, Reymond, Pere, Merienne, & Kemeny, 2008). Rendering low frequency accelerations in a limited workspace is achieved to a great extent by the "tilt coordination" technique that takes advantage of the perceptual ambiguity of the otolith organs between sustained linear accelerations and rotation (Berger, Schulte-Pelkum, & Bültoff, 2010; Groen & Bles, 2004). The technique consists in stimulating the otolith organs by the means of changing the gravitoinertial force to produce an illusion of linear motion.

In literature, a large number of research efforts using simulators address curve driving (e.g. Charlton, 2004; Comte & Jamson, 2000; Coutton-Jean et al., 2009; Mulder et al., 2008). Nevertheless, few have reported on developing and characterizing simple and efficient methods to be used when mainly lateral cues are needed.

Under the above perspective, this work intends to contribute on developing a simple methodology to achieve successful rendering of characteristic lateral accelerations of curve negotiation within the constrained workspace of a Stewart Platform only by tilt coordination.

II.2 Method

II.2.1 Main considerations for the proposed method

As stated in previous technical and scientific literature, a requirement for the tilt coordination method to properly render sustained linear acceleration illusion is to perform rotation under the semicircular canals detection threshold, i.e. about 3°/s as

stated by Groen & Bles (2004) and utilized by several authors (e.g. Berger et al., 2010; Liao, Chih-Fang, & Chieng, 2004). However, some tests performed with higher rotational speeds, report no significant deterioration of the perceptual validity of the simulation (e.g. Feenstra, Wentink, Roza, & Bles, 2007; Valente-Pais, Wentink, Paassen, & Mulder, 2009).

Also, it has been stated that one-to-one restitution of motion cues is not necessary to successfully achieve perceptual validity (e.g. Dagdelen, Reymond, & Kemeny, 2002; Kemeny, 2001; Siegler et al., 200;). Downscaling and approximating the original acceleration cues are resources often utilized when simulating since most of the motion devices have very limited workspace (e.g. Damveld et al., 2010; Freeman, Watson, Papelis, Lin, Tayyab, Romano et al., 1995; Greenberg et al., 2003).

Another consideration is to maintain a coherent visual input in terms of reference and visual acceleration (e.g. Berger et al., 2010; Kemeny, 1999). This minimizes motion sickness and produce vection (illusion of self-motion by visual input) that enhances the simulation. This aspect in particular will be assumed but not treated directly as part of the method proposed.

II.2.2 Apparatus

A 6 universal-prismatic-universal (UPU) electromechanical Stewart Platform is used to produce the motion cues. The platform was designed and built at the Department of Mechanical Engineering of Pontificia Universidad Católica de Chile as a first step to experimenting in generating low cost, yet realistic immersive simulations for training drivers of heavy machinery as used in mining, construction and forest industries.

Platform dimensions are 450 mm base radius, 350 mm top radius and 760 mm height in home position. The 200 mm stroke of the linear actuators allows platform motion ranges of ± 22 cm for surge/sway movements, ± 10 cm for heave

displacement, ± 20° for roll/pitch tilting and ± 40° for yaw rotation as illustrated schematically in **Figure II.1**. Linear and angular accelerations reach up to 40 cm/s^2 and 100 °/s^2 respectively. A payload of 300 kg can be supported.

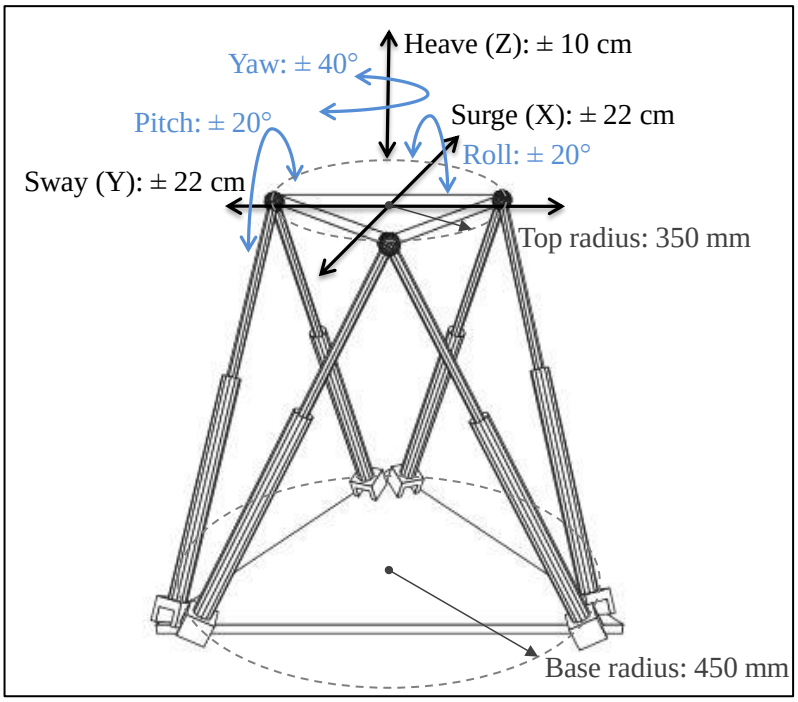

Figure II.1: Degrees of freedom of a Stewart Platform manipulator.

The linear actuators are driven by 24V PMDC motors and their velocity is controlled by PWM signals with a Microchip® processor that receives instructions from a PC at 20Hz. **Figure II.2** shows the scheme of the apparatus with a car seat on top as used for this research.

Figure II.2: Scheme of the apparatus built for the research equipped with a driver's seat.

II.2.3 Tilt coordination method

II.2.3.1 Kinematics

As the objective is to produce linear accelerations only with tilt motion, the required movement of the Stewart Platform is either roll (*x* axis rotation) for lateral accelerations or pitch (*y* axis rotation) for longitudinal accelerations. In this research, only lateral acceleration rendering will be addressed, so, when referring to rotation, it will mean rotation in the *x* axis.

We want to derive an expression for the acceleration in the axis passing from ear to ear of the subject sitting on the motion device, referred as interaural axis, to determine which will be the input of the otolith organs of the vestibular system.

For the kinematic analysis, a base reference frame is positioned at the center of the moving platform at point A. Also, a second reference frame, integral to the vestibular system of a person on the seat, is chosen to be in the longitudinal plane of symmetry at a configurable distance *r* above point A. **Figure II.3** shows the base (0) and auxiliary (1) reference frames defined for the analysis as well as the positive direction of rotation.

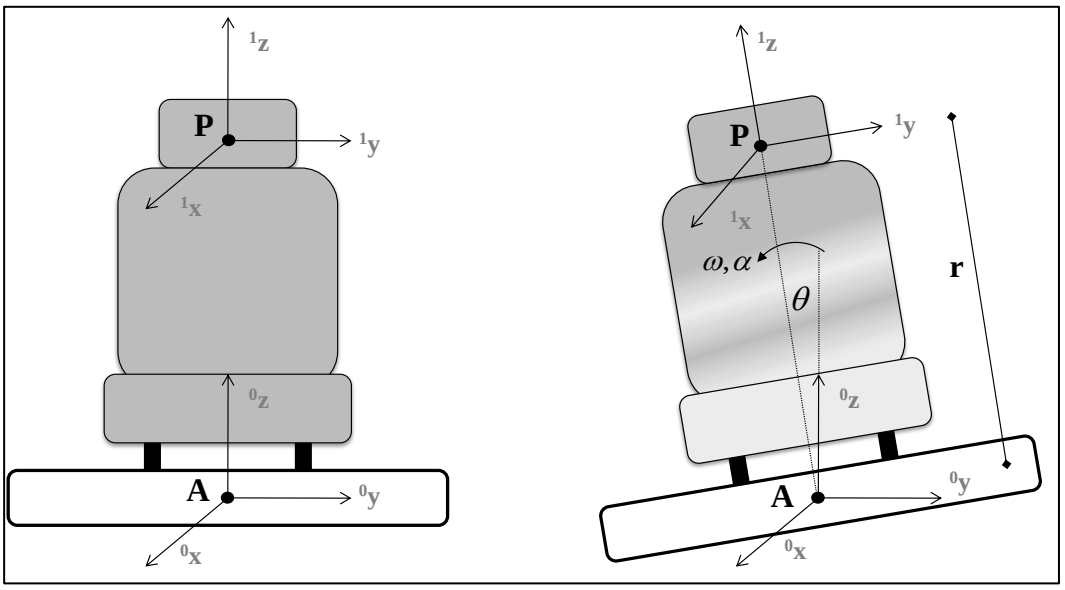

Figure II.3: Kinematic analysis of the vestibular system location (point P) during pure rotation of the platform.

Acceleration of point P is given by:

$$\vec{a}_P = \vec{a}_A + \vec{\alpha} \times \vec{r}_{AP} + \vec{\omega} \times (\vec{\omega} \times \vec{r}_{AP}) \qquad \text{(Eq.1)}$$

Where $\vec{a}_A$ is the absolute acceleration of the center of the platform, $\vec{\alpha}$ the platform absolute angular acceleration, $\vec{\omega}$ its absolute angular velocity and $\vec{r}_{AP}$ the relative position of point *P* from the base reference frame origin (point *A*).

Considering only rotation around the *x* axis, we have:

$$\vec{a}_A = -g \cdot {}^0\hat{k}$$

$$\vec{\omega} = -\dot{\theta} \cdot {}^0\hat{\imath}$$

$$\vec{\alpha} = \dot{\vec{\omega}} = \ddot{\theta} \cdot {}^0\hat{\imath}$$

$$\vec{r}_{AP} = r \cdot {}^0\hat{k}$$

Then, acceleration of point *P* has the following expression:

$${}^0\vec{a}_P = -g \cdot {}^0\hat{k} + \left(\ddot{\theta} \cdot {}^0\hat{\imath}\right) \times \left(r \cdot {}^0\hat{k}\right) \qquad \text{(Eq.2)}$$

Now, expressed in the local reference frame (1) we have:

$${}^1\vec{a}_P = -\left(g \sin\theta + r\ddot{\theta}\right) \cdot {}^1\hat{\jmath} + g \cos\theta \cdot {}^1\hat{k} \qquad \text{(Eq.3)}$$

This means that longitudinal acceleration exerted in the interaural axis is the sum of the sine component of the gravity and the effect of angular acceleration. Change in magnitude in the *z* axis is considered not significant to interfere with perceptual validity of the simulation of lateral cues.

We define:

$$a_{interaural}(t) = g\, sin\, \theta(t) + r\ddot{\theta}(t) \qquad \text{(Eq.4)}$$

Then, to render simulation, $a_{interaural}(t)$ has to be matched as closely as possible with the desired acceleration to produce with the Stewart platform the corresponding stimuli in the vestibular system.

II.2.3.2 Description of the method

The proposed method for simulation by tilt coordination is composed by three main processes: a) the input signal fitting, b) the inverse kinematics and c) the motion rendering with the Stewart Platform. **Figure II.4** shows a flowchart of the processes with theirs inputs and outputs.

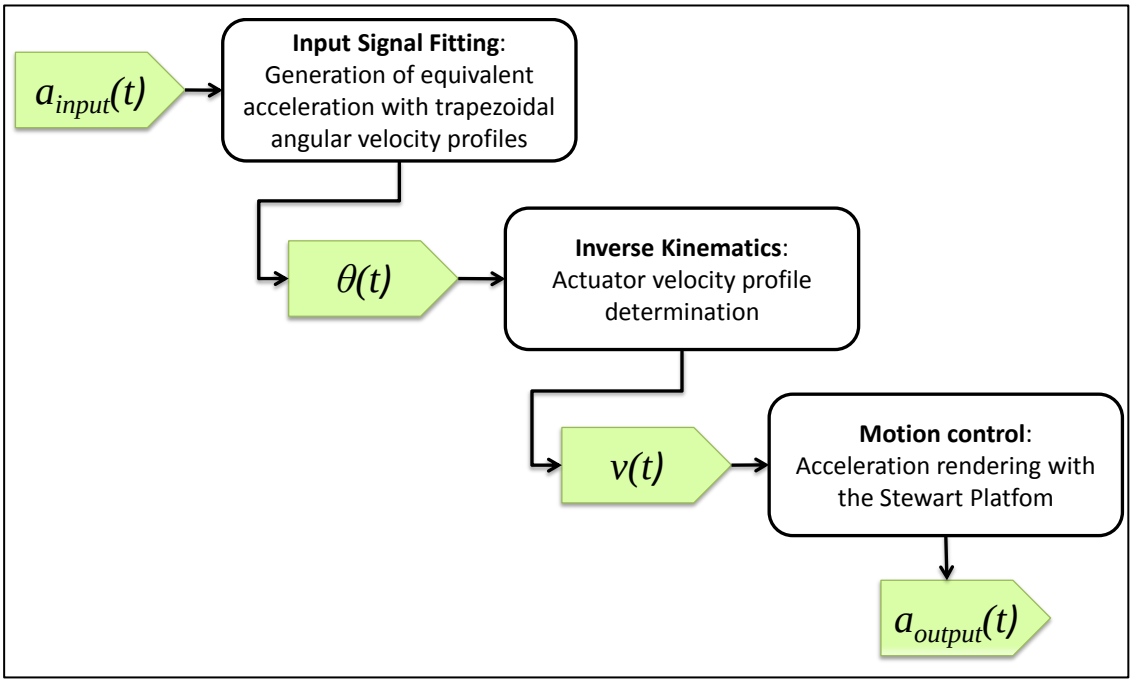

Figure II.4: Flowchart of the proposed method with respective inputs and outputs of each process.

The main input signal is assumed to be a set of linear lateral accelerations of a car with predominant low frequency content; this signal will be referred as $a_{input}(t)$. This acceleration signal corresponds to a register of selected real driving situations or a synthesized history as well.

The first stage of the method is to produce a best fit between $a_{input}(t)$ and $a_{interaural}(t)$ by the means of selecting a proper angular velocity profile $\dot{\theta}(t)$ for the Stewart Platform. For the sake of simplicity and reliability, trapezoidal profiles are used. The profile parameters are: total time $\boldsymbol{T}$, acceleration time $\boldsymbol{t_{acc}}$ (as a % of $\boldsymbol{T}$), deceleration time $\boldsymbol{t_{dec}}$ (as a % of $\boldsymbol{T}$), and maximum angular velocity $\boldsymbol{\omega_{max}}$ as illustrated in **Figure II.5**. Then, the task is to find $\boldsymbol{T}$, $\boldsymbol{t_{acc}}$, $\boldsymbol{t_{dec}}$ and $\boldsymbol{\omega_{max}}$ such that:

$$a_{interaural}(t) \approx a_{input}(t)$$

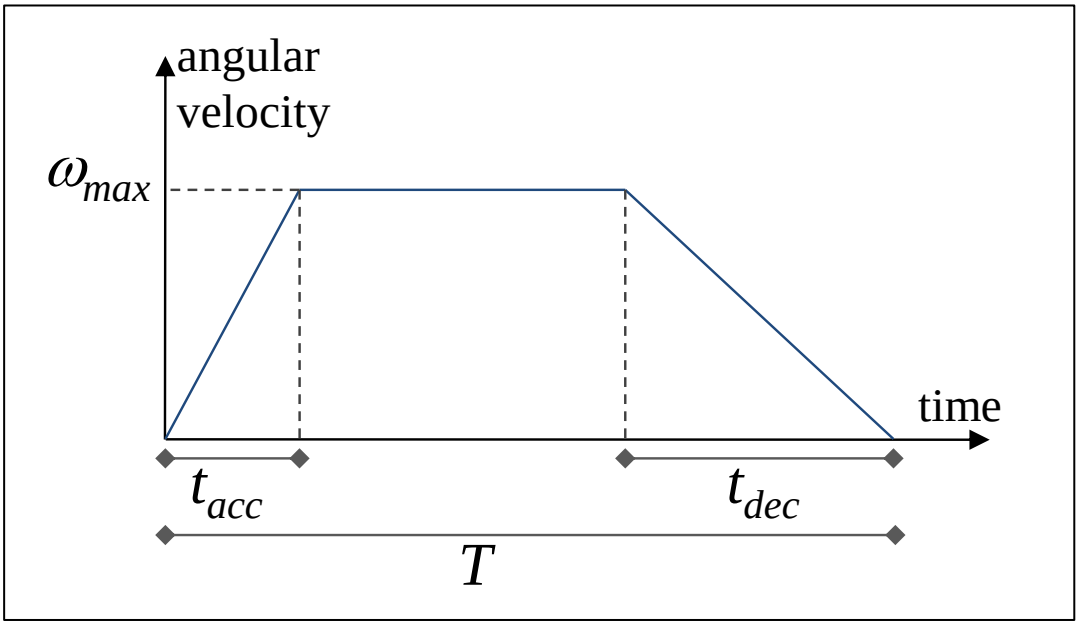

Figure II.5: Generic trapezoidal angular velocity profile defined by 4 parameters: total time, acceleration time, deceleration time and maximum angular rate.

The next step is to produce the velocity profiles of the linear actuators of the Stewart Platform. For this, corresponding $\theta(t)$ from previous step is fed to a MATLAB Simulink model. This model consists in a physical plant with dynamic control to follow a reference trajectory. The physical plant is generated with SimMechanics bodies and connections blocks with the characteristics of the Stewart Platform built for this work. The control uses inverse dynamics and a standard PID controller. The inputs for this model are the values of the six degrees of freedom of the moving platform respect to a fixed reference frame as a function of time. Kinematic and dynamic data as well as a visualization of the platform are obtained as output. Then, $\theta(t)$ is used to synthesize the velocity profiles $\vec{v}(t)$ of the platform linear actuators needed to perform the motion for simulation. The main blockset of the Simulink model is presented in **Figure II.6**.

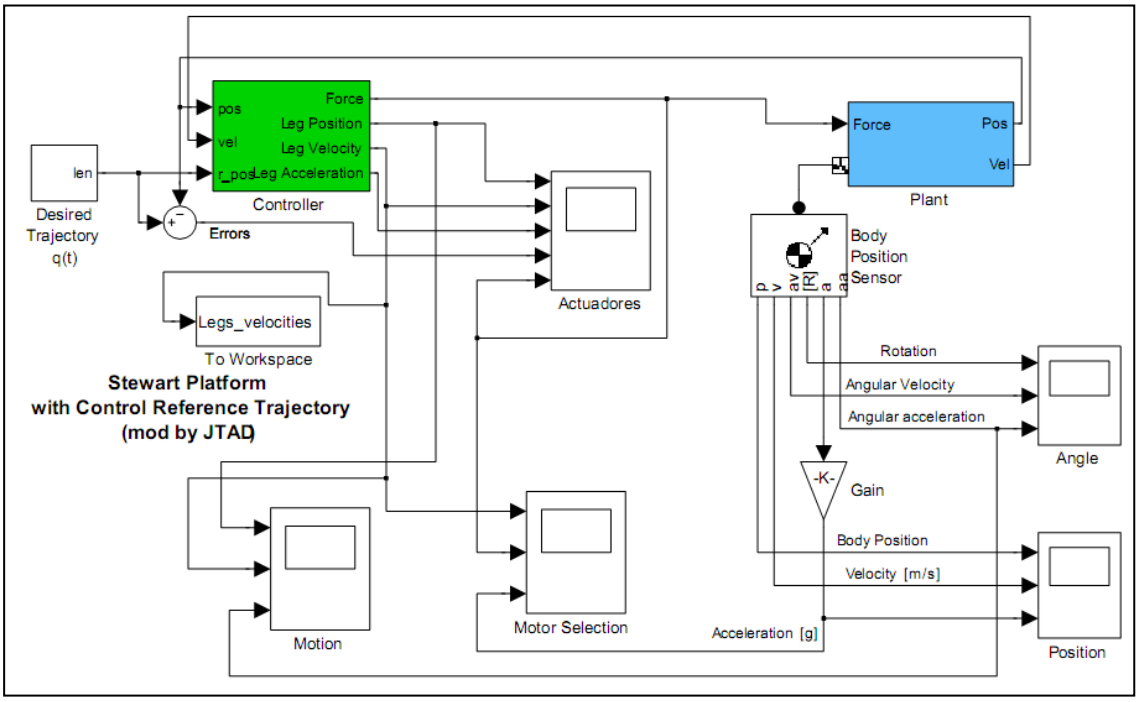

Figure II.6: The blockset for Simulink reference trajectory model of the SP.

Finally, linear velocity reference signal commands are sent from a PC to the platform controller to produce motion. Resulting acceleration during simulation will be referred as $a_{output}(t)$.

II.2.4 Experimental procedures

Three experiments were carried out to asses overall performance of the simulation with the Stewart Platform using the proposed methodology. The first experiment is a benchmark for the proposed method, the second addresses real driving data and the third focuses on enhancing rendering capabilities of the methodology.

II.2.4.1 Experiment 1

During this experiment, a "synthetic" set of accelerations was simulated as a benchmark to measure the quality of the motion platform and its controller. An arbitrary set of parameters for $\dot{\theta}(t)$ was selected to obtain input signal $a_{interaural}(t)$.

Table II.1 presents the chosen arbitrary parameters **Figure II.7** shows the corresponding interaural acceleration. Resulting cues during motion are compared with the input signal in terms of absolute and mean square errors.

Table II.1: Arbitrary parameters chosen for benchmark experiment

Trapezoidal profile parameter	Value (units)
Total time $\boldsymbol{T}$	6 (s)
Acceleration time $\boldsymbol{t_{acc}}$	1.5 (s)*
Deceleration time $\boldsymbol{t_{dec}}$	4.5 (s)**
Maximum angular rate $\mathbf{w}_{\boldsymbol{max}}$	0.09 (rad/s)

* 25% of T ** 75% of T

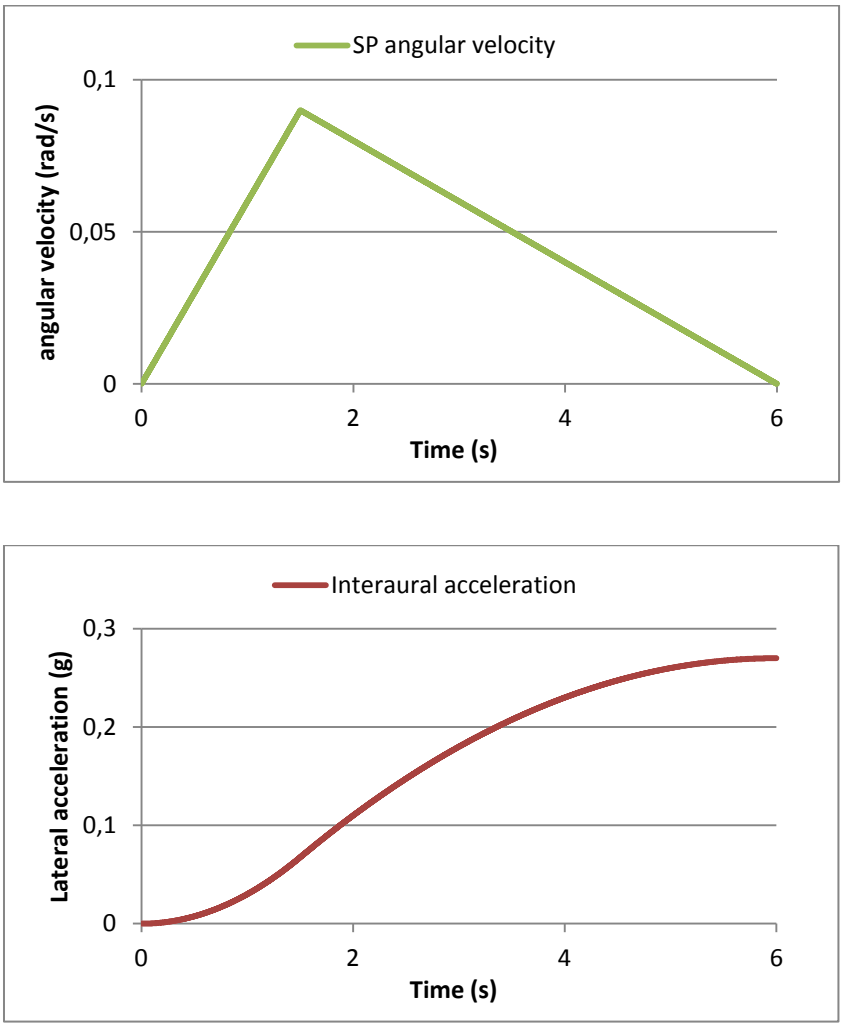

Figure II.7: (Up) Arbitrary generated trapezoidal velocity profile for benchmark experiment. (Down) Resultant interaural acceleration used as reference input signal.

II.2.4.2 Experiment 2

The objective of the second experiment was to test the capability of the method to accomplish one-to-one rendering of a real world situation according to the characteristics of the method and the limitations of the Stewart Platform.

Real acceleration data was recorded during urban driving as input signal for simulation. The selected scenario is a roundabout located in the city of Santiago,

Chile. The driving consisted in entering the roundabout from a tangent entry at constant speed until reaching the maximum curvature and keeping a sustained lateral acceleration. **Figure II.8** shows an aerial view of the selected roundabout and the trajectory divided in a straight approach, a transition to the final curvature and an idealized circular path. Processed lateral acceleration data was used as input signal for the method.

Figure II.8: Aerial view of the roundabout for experimental data collection. Straight entry (blue), transition curve (red) and final circular path (green) are shown.

II.2.4.3 Experiment 3

In the third experiment, two techniques were incorporated to expand the capabilities of simulation of the proposed method. One was downscaling the input signal, a broadly used strategy because the difficulty of motion devices to perform one-to-one rendering. The second was to transgress the rotational perception threshold of the semicircular canals, i.e. increase the maximum rotational velocity from 3 to 6 °/s, to perform faster movements and thereby expand the motion rendering capabilities.

The input signal was derived from a kinematic model of a car drift. The selection of this situation has a twofold reason: a) it is a demanding event in terms of acceleration and b) the situation has a risk component that makes preferable not to generate real life measurements for simulation. Basically, the drift is modeled by considering a deviation from the original curve trajectory and an additional spin of the vehicle. An illustration of the drift model is shown in **Figure II.9** separated in four phases. Phase A corresponds to initial normal curve negotiation. In phase B, drift starts causing the car to lose the original trajectory and its tangential orientation. Then, in phase C, spin is controlled but curve negotiation occurs while not heading tangential to the path. Finally, in phase D, a corrective turn brings back the car to the correct heading.

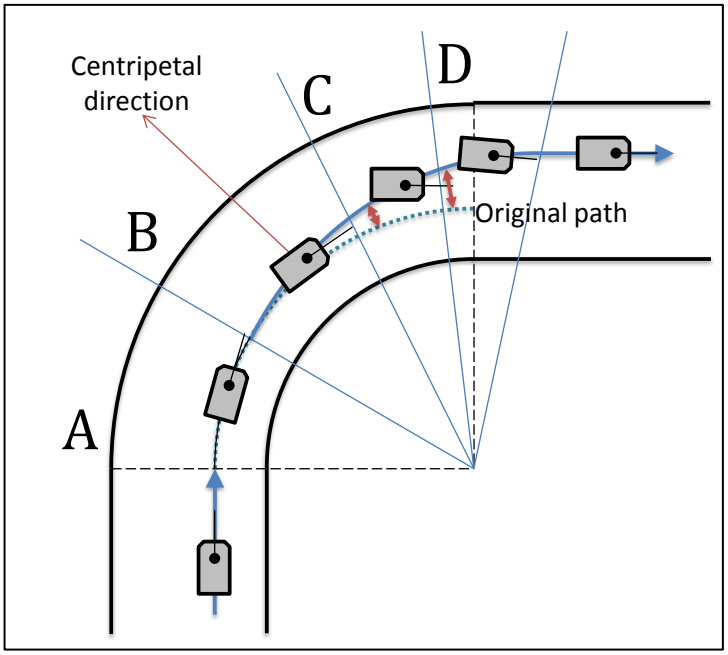

Figure II.9: Car drift modeled in 4 phases. First, normal curve negotiation (A); then, drift starts (B); after spin stops, not tangential curve negotiation occurs (C); finally, the vehicle returns to tangential heading (D).

Initially, a set of accelerations corresponding to a normal 90° curve of 50 m radius at 50 km/h were considered as a starting point to calculate lateral acceleration during drift. Angular yaw rate and resulting net lateral acceleration of the vehicle is shown in **Figure II.10** considering spin due to drift during phase B and correction of heading in phase D. Then, net interaural acceleration is affected by an additional angular acceleration and misaligning of this axis respect to centripetal direction. Downscaled signal (50% of original) used as reference input for simulation is shown in **Figure II.11**.

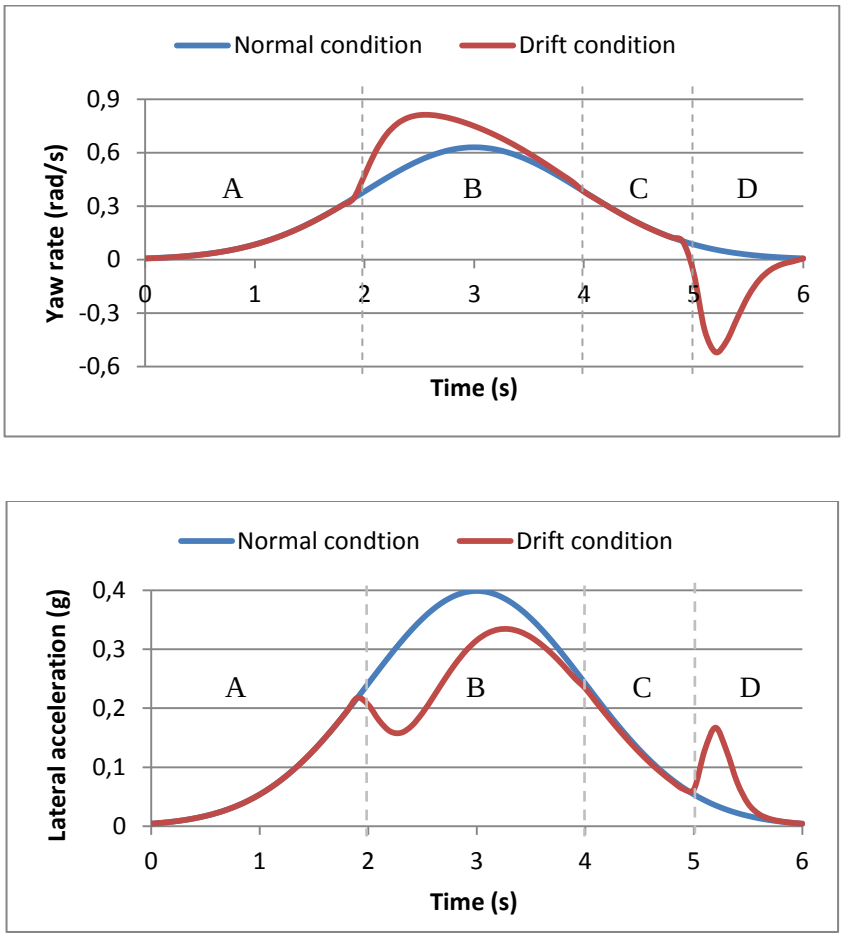

Figure II.10: Yaw rate (Up) and net interaural acceleration (Down) during drift. Phases B and D have notorious differences with respect to normal curve negotiation.

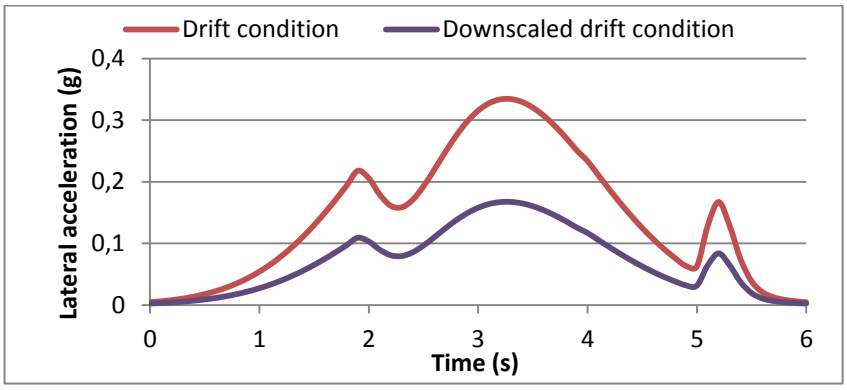

Figure II.11: Non-scaled and downscaled net interaural acceleration during drift. Downscaling decreases significantly the demand of high tilt rates and rotations.

II.2.5 Data recording and analysis

A STMicroelectronics LIS302DL 3-axis accelerometer with ± 2.0 g range and sampling frequency of 100 Hz was used for measurements during experimental driving and motion rendering with the Stewart Platform.

For experimental data collection used for reference signal generation, the unit was placed in the plane of symmetry of a car (a 1,665 kg gross weight Chevrolet Optra) on the front panel. Lateral and longitudinal acceleration data was recorded at 100 Hz. Measurements initiated when constant speed was reached in the straight entry and finished after 2-3 seconds of sustained constant lateral acceleration. The signals were passed through a second order low-pass Butterworth filter at 1 Hz. No significant difference due to the positioning of the accelerometer with respect to the driver's head was considered. Longitudinal data was recorded but not utilized in this research.

Recording of the Stewart Platform accelerations was done at 100 Hz. The accelerometer was positioned 70 cm above the moving platform where the otolith organs of the vestibular system would be. This data was also passed through a second order low-pass Butterworth at 1 Hz for later comparison with desired input acceleration.

II.3 Results and discussion

II.3.1 Experiment 1

Resulting raw and low passed accelerations of the Stewart Platform measured during simulation are graphically compared with reference input data in **Figure II.12**. Absolute and mean square errors for both comparisons are resumed in **Table II.2**.

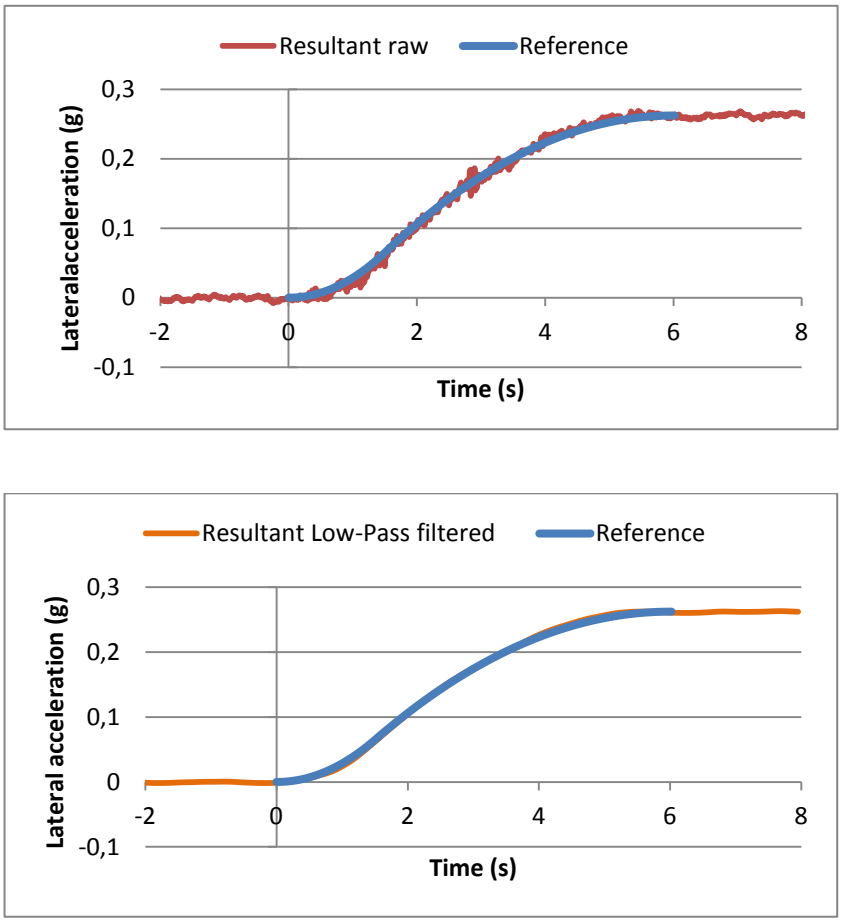

Figure II.12: (Up) Comparison between reference and resultant raw accelerations. (Down) Comparison between reference and low passed resultant accelerations.

Table II.2: Differences between resultant and reference acceleration in benchmark experiment

Measure of comparison (units)	Raw	Low-passed
Mean squared error (g)	0.6E-2	0.3E-2
Maximum absolute error (g)	2.2E-02	0.5E-02

Resulting motion cues have minimal differences with the reference signal from the tilt coordination method. Errors range in orders of 10^{-3}-10^{-2} g in both comparisons (raw data and low passed filtered data).

Minimal errors were found and no significant effects of vibration or friction during motion are noticed. Then, the method, the platform and its controller as a whole can be considered valid and reliable for further experimentation.

II.3.2 Experiment 2

Experimental raw lateral acceleration data of the driving session is shown together with the low passed filtered data in **Figure II.13**. The portion of the acceleration to be used as $a_{input}(t)$ corresponding to curve negotiation is indicated in the same graph. More specifically, the low passed filtered data of will be the input.

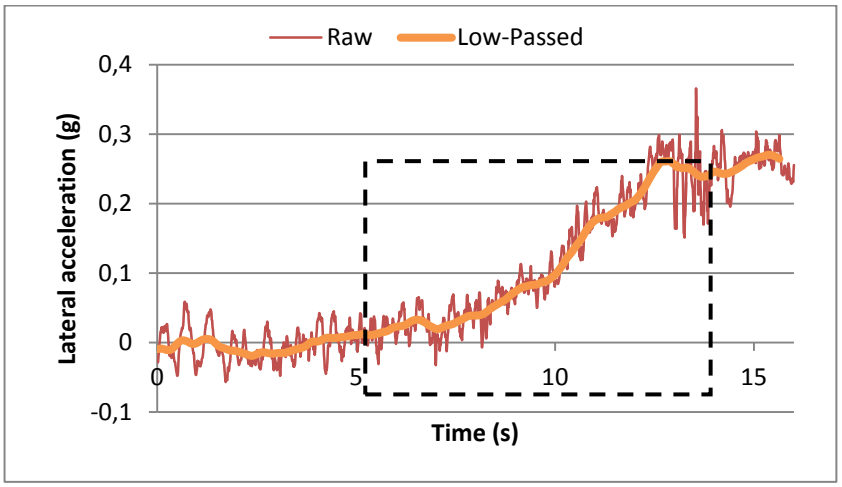

Figure II.13: Experimental data from driving session in the selected roundabout. An increasing lateral acceleration is seen until maximum curvature is reached. The box indicates the part of the data used as reference signal for experiment 2.

We established two conditions for the fit of the input signal: a) mean square error less than 10^{-3} g and b) final angle of the platform correspondent to lateral acceleration due to gravity projection in the interaural axis. **Table II.3** shows the parameters used to fit the interaural acceleration satisfying the above conditions.

Table II.3: Parameters for input signal fitting in real event rendering experiment

Trapezoidal profile parameter	Value (units)
Total time $\boldsymbol{T}$	8.37 (s)
Acceleration time $\boldsymbol{t_{acc}}$	8.37 (s)*
Deceleration time $\boldsymbol{t_{dec}}$	0 (s)**
Maximum angular rate $\mathbf{w}_{max}$	0.06 (rad/s)
* 100% of T	** 0% of T

Figure II.14 shows the resultant motion cues compared with the acceleration reference input. **Table II.4** presents the magnitude of the mean square and absolute errors.

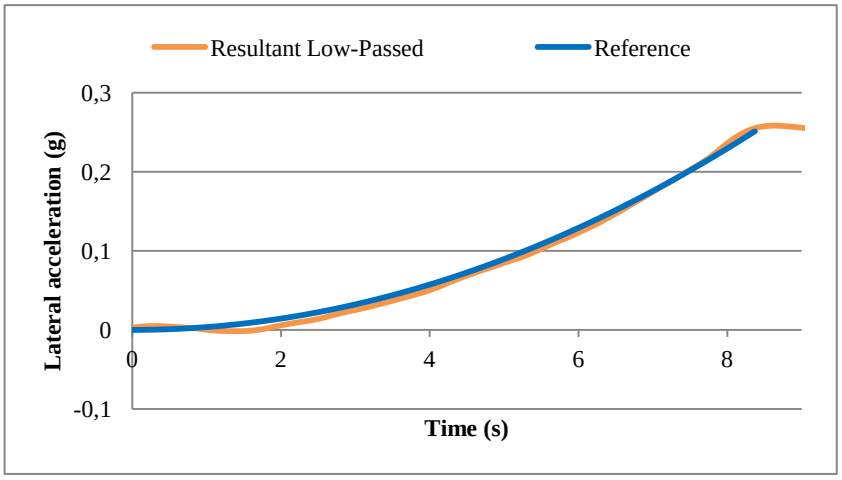

Figure II.14: Comparison of reference and low passed resultant accelerations for experiment 2.

Table II.4: Differences between resultant and reference acceleration in real event rendering experiment

Measure of comparison (units)	Low-passed
Mean squared error (g)	1.1E-02
Maximum absolute error (g)	2.5E-02

In this case, one-to-one rendering was feasible because the real world situation was contained in the capabilities of the motion device and method. In terms of physical validity, the small error during motion indicates that the desired cues were properly rendered. Squared error remained below the order of 10^{-4} g during the whole motion while mean squared error resulted about an order of magnitude below the established value in the conditions for the fit. Also, the terminal platform angle satisfied the magnitude of the final sustained lateral acceleration of the roundabout which ultimately produces the vestibular system deception.

II.3.3 Experiment 3

Figure II.15 shows the reference input signal and the obtained fit. In this case, the fitting was done by parts because of the change in direction of angular velocity. **Table II.5** resumes the parameters used for each part. The condition for the fit was to minimize the squared error in each part using tilt rates up to 6°/s.

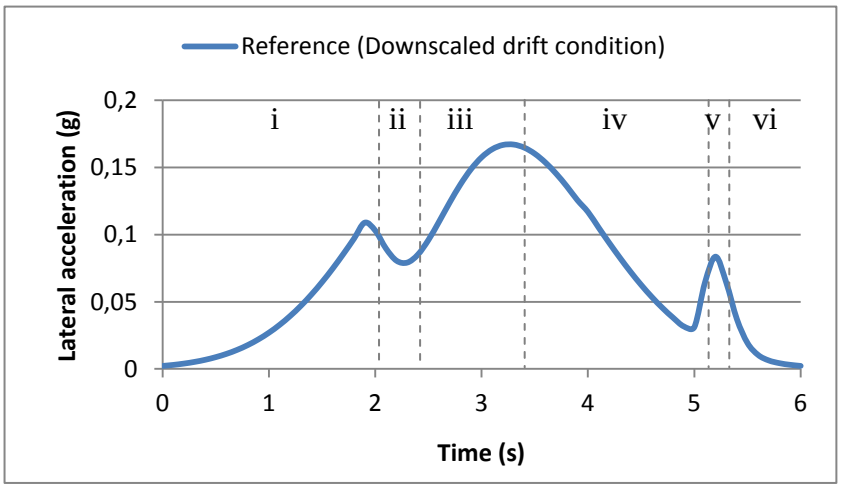

Figure II.15: Downscaled reference input signal of drift model and obtained signal fit. The need of bidirectional rotations force to partition the movement in 6 sections.

Table II.5: Parameters for input signal fitting in experiment 3.

Part i	Value (units)
Total time $\boldsymbol{T}$	1.9 (s)
Acceleration time $\boldsymbol{t_{acc}}$	1.33 (s)
Deceleration time $\boldsymbol{t_{dec}}$	0 (s)
Maximum angular rate $\mathbf{w}_{max}$	0.085 (rad/s)

Part ii	Value (units)
Total time $\boldsymbol{T}$	0.4 (s)
Acceleration time $\boldsymbol{t_{acc}}$	0.12 (s)
Deceleration time $\boldsymbol{t_{dec}}$	0.12 (s)
Maximum angular rate $\mathbf{w}_{max}$	-0.085 (rad/s)

Part iii	Value (units)
Total time $\boldsymbol{T}$	1 (s)
Acceleration time $\boldsymbol{t_{acc}}$	0 (s)
Deceleration time $\boldsymbol{t_{dec}}$	0.4 (s)
Maximum angular rate $\mathbf{w}_{max}$	0.085 (rad/s)

Part iv	Value (units)
Total time $\boldsymbol{T}$	1.7 (s)
Acceleration time $\boldsymbol{t_{acc}}$	0.34 (s)
Deceleration time $\boldsymbol{t_{dec}}$	0.34 (s)
Maximum angular rate $\mathbf{w}_{max}$	-0.085 (rad/s)

Part v	Value (units)
Total time $\boldsymbol{T}$	0.2 (s)
Acceleration time $\boldsymbol{t_{acc}}$	0 (s)
Deceleration time $\boldsymbol{t_{dec}}$	0 (s)
Maximum angular rate $\mathbf{w}_{max}$	0.085 (rad/s)

Part vi	Value (units)
Total time $\boldsymbol{T}$	0.8 (s)
Acceleration time $\boldsymbol{t_{acc}}$	0 (s)
Deceleration time $\boldsymbol{t_{dec}}$	0.44 (s)
Maximum angular rate $\mathbf{w}_{max}$	-0.085 (rad/s)

Figure II.16 shows resultant low pass filtered accelerations and the reference input signal. **Table II.6** resumes the magnitude of the mean square and absolute errors.

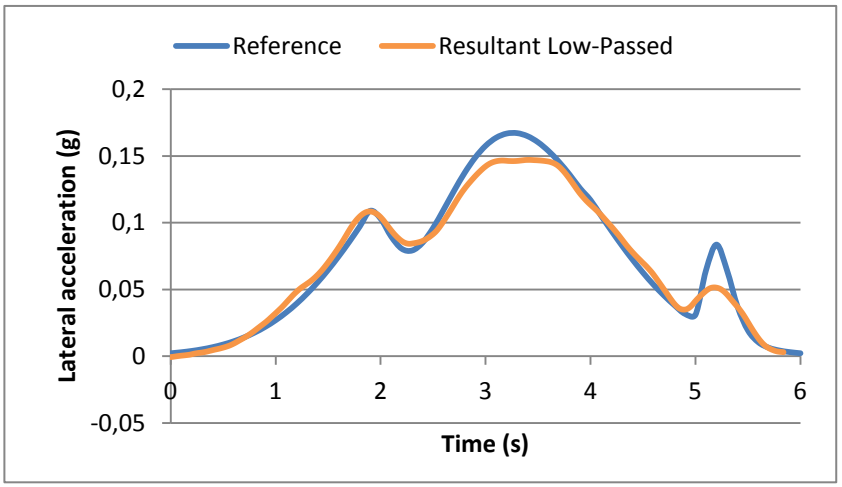

Figure II.16: Comparison of reference and low passed resultant accelerations for experiment 3.

Table II.6: Differences between resultant and reference acceleration in drift model experiment

Measure of comparison (units)	Low-passed
Mean squared error (g)	0.9E-02
Maximum absolute error (g)	1.3E-02

The enhanced method shows good results in terms of physical validity with squared errors in the order of 10^{-3} g. However, perceptual validity can only be assured by testing with human subjects.

The peak accelerations were not intentionally met by the means of sudden change in velocity direction. This effect was not considered in the method but resulted useful to approach to the cues that were still out of reach of the spectrum of simulation.

II.4 Conclusions and future work

In this work, a robust, straightforward and efficient methodology to synthesize the movement of a Stewart Platform to simulate lateral acceleration by tilt coordination has been developed and proved to be effective given different sets of acceleration inputs. It uses trapezoidal angular velocity profiles to best fit a desired acceleration input to be followed. The trapezoidal profiles are processed to generate the individual actuators velocity reference signals which will produce the resultant Stewart Platform motion.

Since errors between resultant and input accelerations ranged in order of 10^{-2} g, satisfactory physical validity of rendered cues was obtained. Hence, good perceptual validity is expected considering that human body does a subjective rating of the sensation and slight deviations doesn't affect at all the deception to the vestibular system. Characteristics inherent of the Stewart Platform parallel manipulator as rigidity and load to force ratio were key to achieve the quality of the simulation results without significant drawbacks for the implemented open loop control.

Effective spectrum of simulation can be vastly enhanced when scaling the input signal and using higher tilt rates than traditional 3°/s. As literature suggests, both techniques does not affect significantly the perception validity depending on the situation so this methodology may be extended to a very broad range of simulation.

This method can be used to render characteristic lateral cues of car driving, limited by the physical capabilities of the moving platform which determines the maximum lateral acceleration that can be simulated. Also, under this approach, as the inputs of the inverse kinematic model utilized are independent, more elaborated movements can be achieved combining longitudinal or rotational cues. The capability to simulate this kind of event benefits behavioral studies that address car driving, delivering a more complete simulation experience supporting sensorial immersion.

Futures perspectives are focused in addressing more sophisticated acceleration events to be simulated with the Stewart Platform. The aim is to develop simple methodologies to characterize and simulate situations as rough terrain driving, inclined roads, sudden braking, etc. considering limited workspace of the motion platform. In the same line, future work will consist in setting up complete driving simulator with a closed-loop controller, a visual system and haptics to be used for training heavy machinery drivers.

REFERENCES

Auberlet, J.-M., Pacaux, M.-P., Anceaux, F., Plainchault, P., & Rosey, F. (2010). The impact of perceptual treatments on lateral control: A study using fixed-base and motion-base driving simulators. *Accident Analysis and Prevention , 42*, 166–173.

Ay, S., Vatandas, E., & Hacioglu, A. (2009). The effect of radius of joint location on workspace analysis of the 6-6 Stewart Platform Mechanism. *4th International Conference on Recent Advances in Space Technologies*, (pp. 728-731). Istanbul.

Benson, A. (1990). Sensory functions and limitations of the vestibular system. In A. W. R. Warren, *Perception and control of self-motion* (pp. 145-170). Hillsdale, NJ: Erlbaum.

Berger, D., Schulte-Pelkum, J., & Bültoff, H. (2010). Simulating Believable Forward Accelerations on a Stewart Motion Platform. *Transactions on Applied Perception , 7* (1), 1-26.

Bowen, S. A., Oakley, B. P., & Barnett, J. S. (2006). *Effects of Motion on Skill Acquisition in Future Simulators.* Report, U.S. Army Research Institute forthe Behavioral and Social Sciences, Department of the Army.

Brookhuis, K. A., & de Waard, D. (2010). Monitoring drivers' mental workload in driving simulators using physiological measures. *Accident Analysis and Prevention , 42*, 898–903.

Charlton, S. G. (2004). Perceptual and attentional effects on drivers' speed selection at curves. *Accident Analysis and Prevention , 36*, 877–884.

Chiew, Y., Abdul Jalil, M., & Hussein, M. (2009). Motion Visualisation And Control Of A Driving Simulator Motion Platform. *Proceeding of the 6th International Symposium on Mechatronics and its Applications*, (pp. 1-5).

Colombet, F., Dagdelen, M., Reymond, G., Pere, C., Merienne, F., & Kemeny, A. (2008). Motion Cueing: What Is The Impact On The Driver's Behavior? *Proceeding of Driving Simulation Conference DSC 2008*, (pp. 171-182). Monaco.

Comte, S., & Jamson, A. (2000). Traditional and innovative speed-reducing measures for curves: an investigation of driver behaviour using a driving simulator. *Safety Science , 36*, 137-150.

Coutton-Jean, C., Mestre, D. R., Goulon, C., & Bootsma, R. J. (2009). The role of edge lines in curve driving. *Transportation Research Part F* , 483–493.

Dagdelen, M., Reymond, G., & Kemeny, A. (2002). Analysis of the visual compensation in the Renault Driving Simulator. *Proceedings of the Driving Simulation Conference 2002*, (pp. 109-119). Paris.

Damveld, H. J., Bonten, J., Happee, R., Paassen, M. v., & Mulder, M. (2010). Motion filter design for driver observation in hexapod car simulators. *Proceedings of the IEEE International Conference on Systems, Man and Cybernetics*, (pp. 1344-1351). Istanbul.

Dasguptaa, B., & Mruthyunjaya, T. (2000). The Stewart platform manipulator: a review. *Mechanism and Machine Theory , 35* (1), 15-40.

du Plessis, L. J. (1999). *An Optimization Approach to the Determination of Manipulator Workspaces.* Mater of Engineering Thesis, Faculty of Engineering, University of Pretoria, Department of Mechanical Engineering, Pretoria.

Feenstra, P. J., Wentink, M., Roza, Z. C., & Bles, W. (2007). Desdemona, An Alternative Moving Base Design for Driving Simulation. *Proceedings of the Driving Simulation Conference 2007.* Iowa City.

Freeman, J., Watson, G., Papelis, Y., Lin, T., Tayyab, A., Romano, R., et al. (1995). *The IOWA Driving Simulator: an implementation and application overview.* SAE Technical Paper Series.

Gough, V. (1965). Communications to: A platform with six degrees of freedom. *Proceedings of the Institution of Mechanical Engineers*, (pp. 379-386).

Gough, V., & Whitehall, S. (1962). Universal tyre test machine. *Proceedings of the 9th International Technical Congress F.I.S.I.T.A*, (pp. 117-137).

Greenberg, J., Artz, B., & Cathey, L. (2003). The Effect Of Lateral Motion Cues During Simulated Driving. *Proceedings of the Driving Simulation Conference 2003.* Dearborn, Michigan.

Groen, E., & Bles, W. (2004). How to use body tilt for the simulation of linear self motion. *Journal of Vestibular Research* , 375–385.

Guo, H., & Li, H. (2006). Dynamic analysis and simulation of a six degree of freedom Stewart platform manipulator. *Proceedings of the Institution of Mechanical Engineers*, (pp. 61-72).

Harris, L. R., Jenkin, M., Zikovitz, D., Redlick, F., Jaekl, P., Jasiobedzka, U., et al. (2001). *Simulating self motion I: cues for the perception of motion.* Research, York University, Departments of Computer Science, Psychology and Psychology, Toronto.

Hostens, I., Anthonis, J., & Ramon, H. (2005). New design for a 6 dof vibration simulator with improved reliability and performance. *Mechanical Systems and Signal Processing* (19), 105-122.

Hua, C., Weishan, C., & Junkao, L. (2007). Optimal Design of Stewart Platform Safety Mechanism. *Chinese Journal of Aeronautics* (20), 370-377.

Huang, C.-I., Chang, C.-F., Yu, M.-Y., & Fu, L.-C. (2004). Sliding-Mode Tracking Control of the Stewart Platform. *5th Asian Control Conference*, (pp. 562-569). Melbourne.

Huang, T., Wuang, J., & Whitehouse, D. (1999). Theory and methodology for kinematic design of Gough-Stewart platforms. *Science in China , 42* (4), 425-436.

Indrawanto, A. (2009). Design and Control of the Stewart Platform Robot. *Third Asia International Conference on Modelling & Simulation*, (pp. 475-480).

Jakobovic, D., & Budin, L. (2002). Forward Kinematics of a Stewart Platform Mechanism. *Proceeding of the 6th Conference on Intelligent Engineering Systems*, (pp. 146-154).

Kemeny, A. (2001). Recent developments in visuo-vestibular restitution of self-motion in driving simulation. *Proceedings of the Driving Simulator Conference 2001*, (pp. 15-18). Sophia Antipolis.

Kemeny, A. (1999). Simulation and perception. *Proceedings of the Driving Simulation Conference 1999*, (pp. 33–55). Paris.

Kemeny, A., & Panerai, F. (2003). Evaluating perception in driving simulation experiments. *TRENDS in Cognitive Sciences , 7* (1), 31-37.

Kim, J.-H., Lee, W.-S., Park, I.-K., Park, K.-K., & Cho, J.-H. (1997). A Design and Characteristic Analysis of the Motion Base for Vehicle Driving Simulator. *IEEE International Workshop on Robot and Human Communication*, (pp. 290-294).

Lee, H. C., Lee, A. H., Camerona, D., & Li-Tsang, C. (2003). Using a driving simulator to identify older drivers at inflated risk of motor vehicle crashes. *Journal of Safety Research* , 453– 459.

Lee, S.-H., Song, J.-B., Choi, W.-C., & Hong, D. (2003). Position control of a Stewart platform using inverse dynamics control with approximate dynamics. *Mechatronics* (13), 605-619.

Liao, C.-S., C.-F. H., & Chieng, W.-H. (2004). A Novel Washout Filter Design for a Six Degree-of-Freedom Motion Simulator. *JSME International Journal , 47,* 626-636.

Lin, J., & Chen, C. (2009). Computer-aided-symbolic dynamic modeling for Stewart-platform manipulator. *Robotica , 27,* 331-341.

Liu, K., Fitzgerald, J. M., & Lewis, F. L. (1993). Kinematic Analysis of a Stewart Platform Manipulator. *Transactions on Industrial Electronics , 40* (2), 282-293.

Liu, M.-J., Li, C.-X., & Li, C.-N. (2000). Dynamics Analysis of the Gough–Stewart Platform Manipulator. *IEEE Transactions on Robotics and Automation , 16* (1), 94-98.

McGehee, D. V., Lee, J. D., Rizzo, M., Dawson, J., & Bateman, K. (2004). Quantitative analysis of steering adaptation on a high performance fixed-base driving simulator. *Transportation Research Part F 7* , 181–196.

Merfeld, D., Zupan, L., & Peterka, R. (1999). Humans use internalmodels to estimate gravity and linear acceleration. *Nature , 398*, 615-618.

Mulder, M., Abbink, D. A., & Boer, E. R. (2008). The effect of haptic guidance on curve negotiation behavior of young, experienced drivers. *IEEE International Conference on Systems Man and Cybernetics*, (pp. 804-809). Singapore.

Nanua, P., Waldron, K., & Murthy, V. (1990). Direct Kinematic Solution of a Stewart Platform. *Transactions On Robotics And Automation , 6* (4), 438-443.

Nehaoua, L., Arioui, H., Espie, S., & Mohellebi, H. (2006). Motion Cueing Algorithms for Small Driving Simulator. *Proceedings of the 2006 IEEE International Conference on Robotics and Automation*, (pp. 3189-3194). Orlando.

Peña, D., Herrera, M., & Quintero, H. (2002). Revisión del estado del arte de manipuladores paralelos. *Scientia et Technica* (42), 81-86.

Preumont, A., Horodinca, M., Romanescu, I., de Marneffe, B., Avraam, M., Deraemaeker, A., et al. (2007). A six-axis single-stage active vibration isolator based on Stewart platform. *Journal of Sound and Vibration* , 644-661.

Ravichandran, K. (2010). Driving simulator for tracked vehicles using Stewart platform manipulator. *International Conference on Emerging Trends in Robotics and Communication Technologies*, (pp. 245 - 249). Chennai.

Reymond, G., & Kemeny, A. (2000). Motion Cueing in the Renault Driving Simulator. *Vehicle System Dynamics* , 249–259.

Reymond, G., Droulez, J., & Kemeny, A. (2002). Visuovestibular perception of self-motion modeled as a dynamic optimization process. *Biological Cybernetics* , 301-314.

Reymond, G., Kemeny, A., Droulez, J., & Berthoz, A. (2001). Role of lateral acceleration in curve driving: Driver model and experiments on a real vehicle and a driving simulator. *The Journal of the Human Factors and Ergonomics , 43* (3), 483-495.

Sevillano, G., Elías, D., Callupe, R., Marcacuzco, R., & Barriga, B. (2008). Gait Simulator Based On The Parallel Stewart-Gough Platform. *Conference on Interdisciplinary Applications of Kinematics.* Lima.

Shanmugaratnam, S., Kass, S. J., & Arruda, J. E. (2010). Age differences in cognitive and psychomotor abilities and simulated driving. *Accident Analysis and Prevention* , 802–808.

Siegler, I., Reymond, G., Kemeny, A., & Berthoz, A. (2001). Sensorimotor integration in a driving simulator: contributions of motion cueing in elementary driving tasks. *Proceedings of the Driving Simulation Conference 2001*, (pp. 33-55). Paris.

Slob, J. (2008). *State-of-the-Art Driving Simulators, a Literature Survey.* Eindhoven: Eindhoven University of Technology, Department Mechanical Engineering Control Systems Technology Group.

Stewart, D. (1965). A platform with six degrees of freedom. *Proceedings of the Institution of Mechanical Engineers*, *180*, pp. 371-386.

Valente-Pais, A. R., Wentink, M., Paassen, M. M., & Mulder, M. (2009). Comparison of Three Motion Cueing Algorithms for Curve Driving in an Urban Environment. *Presence , 18* (3), 200-221.

Wood, S. J., & Reschke, M. F. (2007). Tilt and translation motion perception during off-vertical axis rotation. *Experimental Brain Research , 182* (3), 365–377.

Zhang, Z., Zhao, D., & Chen, T. (2007). Master-Slave Manipulators Bilateral Control System with Force Tele-presence. *International Conference on Robotics and Biomimetics*, (pp. 307-311). Sanya, China.

APPENDICES

Appendix A: Drawing of the linear actuator manufactured for the Stewart Platform

Appendix B: Specifications of the PMDC motor used

Z55D

电机外型尺寸

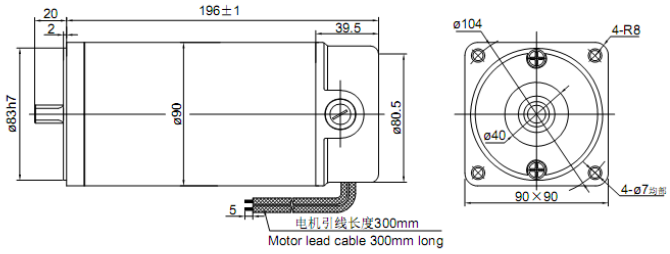

电机性能参数

型号	电压	功率	空载参数		负载参数			电刷寿命	电机重量	备注
			转速	电流	转速	力超	电流			
	(V)	(W)	(RPM)	(A)	(RPM)	(kg.cm)	(A)	(H)	(kg)	
Z55D300-24 □	24	300	3600	2.5	3200	9.14	17.0	2000	5.5	
Z55D300-220 □	220	300	3200	0.5	2800	1.02	1.8	2000	5.5	

电机特性曲线
Characteristic Curve of Motor

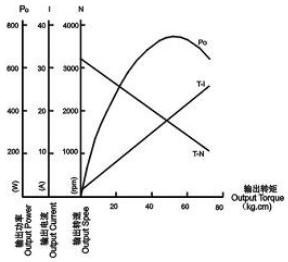

电机接线图
Wiring Diagram of Motor

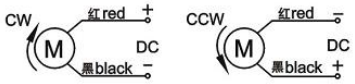

- 标准引出线长度:300mm±10,型号:UL1015规格:AWG14;电机引出线长度、型号在配件尺寸等条件允许的情况下可根据客户要求定制
- Stanclard length of lead wire:300mm±10,model:UL1015 type:AWG14;lead wire length,model will be customerised by dient requestmant under allowed circumstamce of adoptable dimension

Appendix C: Experimental measurements of accelerations in a car

a) Cornering

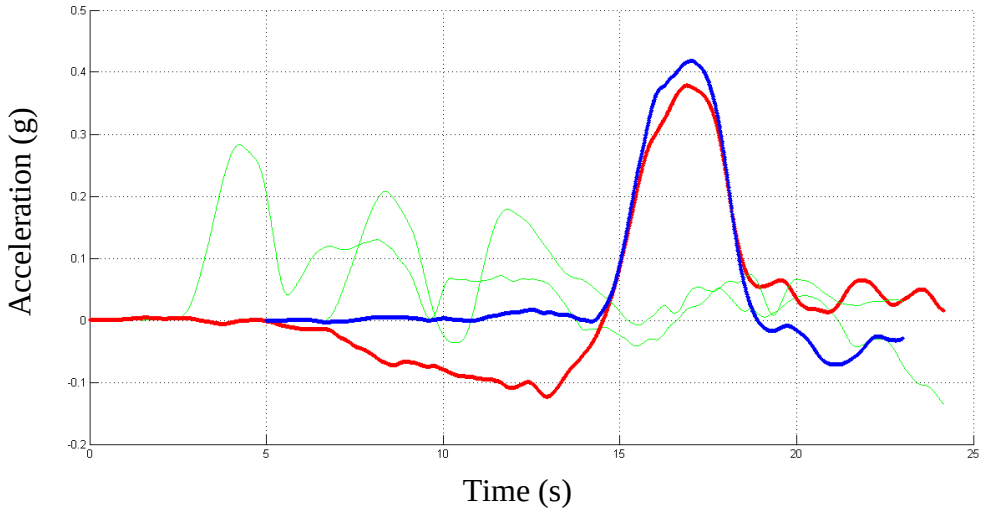

--- : Longitudinal accelerations

--- : Lateral accelerations during cornering experiment 1

--- : Lateral accelerations during cornering experiment 2

b) Accelerating from 0 to 50 km/h

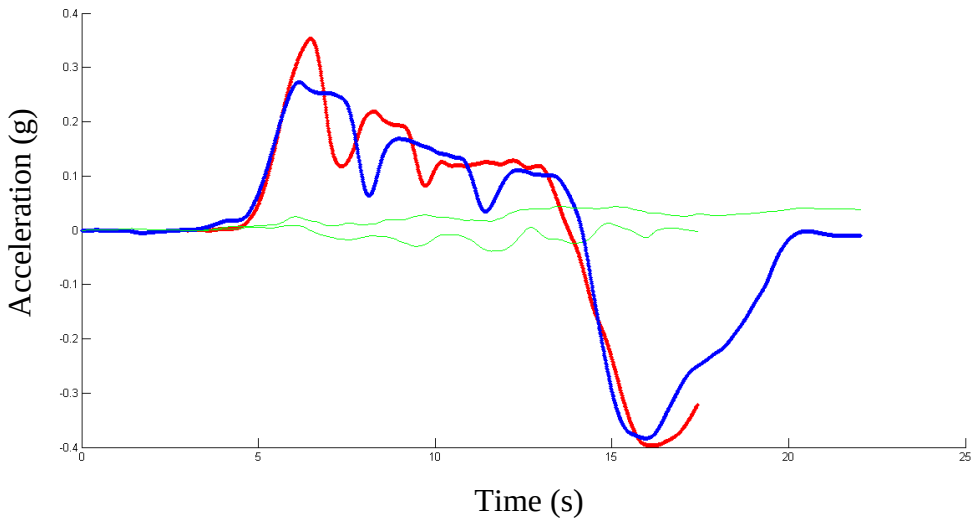

--- : Lateral accelerations

--- : Longitudinal accelerations during acceleration experiment 1

--- : Longitudinal accelerations during acceleration experiment 2

c) Roundabout

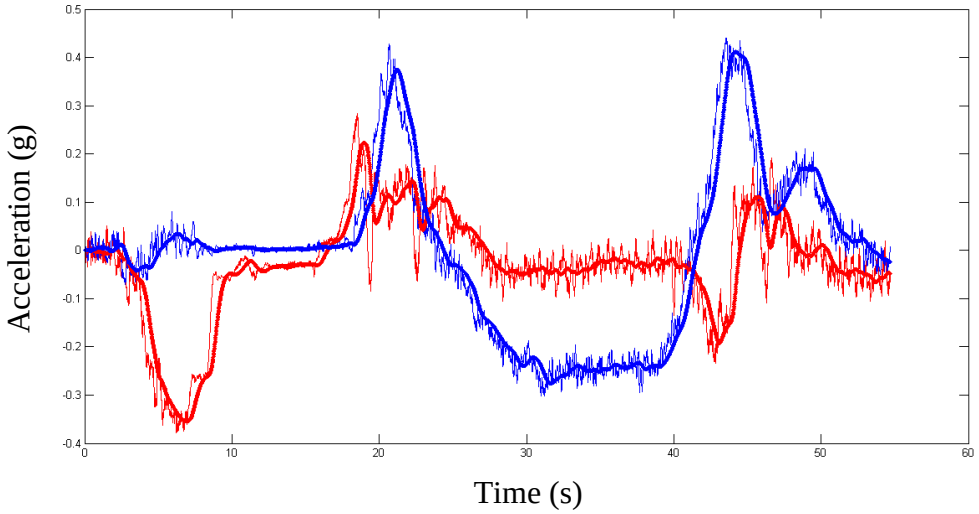

--- : Longitudinal accelerations during roundabout experiment

--- : Lateral accelerations during roundabout experiment

Appendix D: Complete raw and low passed acceleration data from experimental measurement for experiment 2

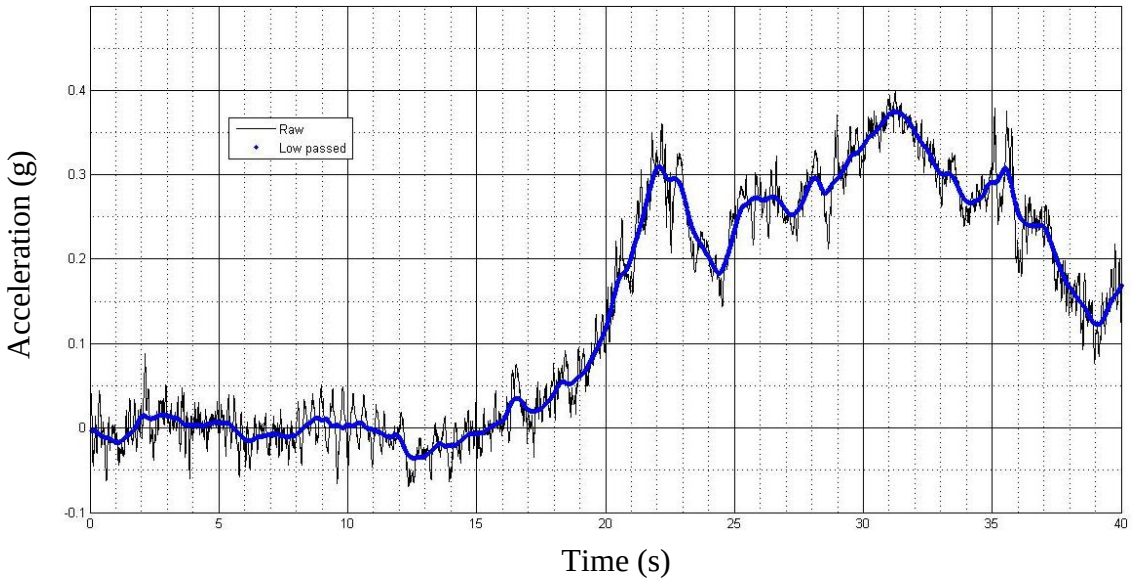

Appendix E: Resultant raw data for each experiment

a) Experiment 1

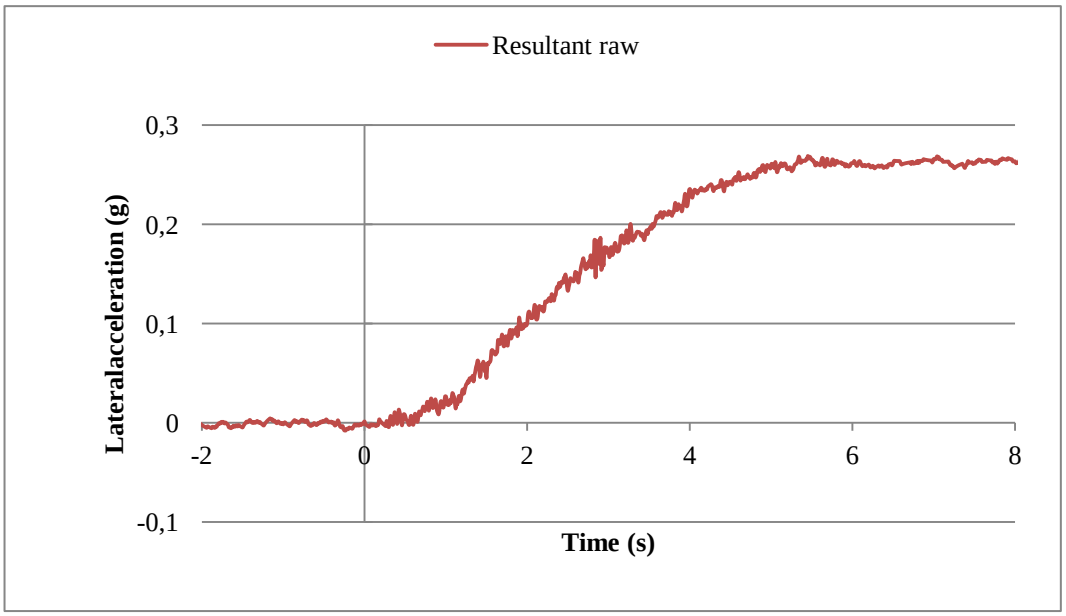

b) Experiment 2

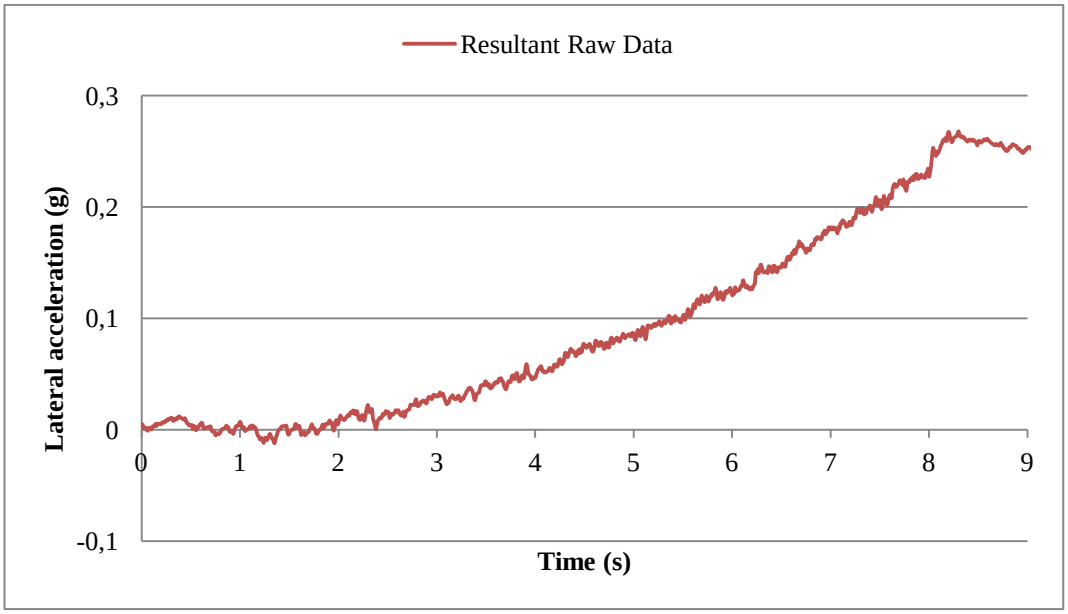

c) Experiment 3